Published in final edited form as:
CNS Neurol Disord Drug Targets. 2013 May 1; 12(3): 413–425.

Neurorestorative Effect of Urinary Bladder Matrix-mediated Neural Stem Cell Transplantation Following Traumatic Brain Injury in Rats

JY Wang[#1], **AKF Liou**[#2], **ZH Ren**[1], **L Zhang**[3], **BN Brown**[4,5], **XT Cui**[3,4,7], **SF Badylak**[4,5], **YN Cai**[1], **YQ Guan**[1], **Rehana K. Leak**[6], **J Chen**[1,2], **X Ji**[1], and **L Chen**[1]

[1]Department of Neurosurgery and China International Neuroscience Institute, Xuanwu Hospital, Capital Medical University, Beijing, China

[2]Center of Cerebrovascular Disease Research, University of Pittsburgh School of Medicine, Pittsburgh, PA 15213, USA

[3]Department of Bioengineering, University of Pittsburgh, Pittsburgh, PA 15261, USA

[4]McGowan Institute for Regenerative Medicine, University of Pittsburgh, PA 15261, USA

[5]Department of Surgery, University of Pittsburgh School of Medicine, Pittsburgh, PA 15261, USA

[6]Division of Pharmaceutical Sciences, Mylan School of Pharmacy, Duquesne University, Pittsburgh, PA 15282, U.S.A.

[7]Center for Neural Basis of Cognition, University of Pittsburgh, Pittsburgh, PA 15261, USA

[#] These authors contributed equally to this work.

Abstract

Traumatic brain injury (TBI) is a leading cause of cell death and disability among young adults and lacks a successful therapeutic strategy. The multiphasic injuries of TBI severely limit the success of conventional pharmacological approaches. Recent successes with transplantation of stem cells in bioactive scaffolds in other injury paradigms provide new hope for the treatment of TBI. In this study, we transplanted neural stem cells (0.5×10^5 cells/μl) cultured in a bioactive scaffold derived from porcine urinary bladder matrix (UBM; 4 injection sites, 2.5μl each) into the rat brain following controlled cortical impact (CCI, velocity, 4.0 m/sec; duration, 0.5 sec; depth, 3.2mm). We evaluated the effectiveness of this strategy to combat the loss of motor, memory and cognitive faculties. Before transplantation, compatibility experiments showed that UBM was able to support extended proliferation and differentiation of neural stem cells. Together with its reported anti-inflammatory properties and rapid degradation characteristics *in vivo*, UBM emerged to be an ideal scaffold. The transplants reduced neuron/tissue loss and white matter injury, and also significantly ameliorated motor, memory, and cognitive impairments. Furthermore, exposure to UBM alone was sufficient to decrease the loss of sensorimotor skills from TBI (examined 3–28

Corresponding Authors: Dr. Ling Chen, Department of Neurosurgery, Xuanwu Hospital of Capital Medical University, 45 Changchun St, Beijing, 100053, China. Tel: +86-10-83198852. chlyz34@163.com or Dr. Xunming Ji, Cerebrovascular Diseases Research Institute, Xuanwu Hospital of Capital Medical University, 45 Changchun St, Beijing, 100053, China. Tel: +86-10-83198129. jixm@ccmu.edu.cn.

days post-CCI). However, only UBMs that contained proliferating neural stem cells helped attenuate memory and cognitive impairments (examined 26–28 days post-CCI). In summary, these results demonstrate the therapeutic efficacy of stem cells in bioactive scaffolds against TBI and show promise for translation into future clinical use.

Keywords

TBI; UBM; stem cell transplantation; protection; neurodegeneration; neurobehavioral function

Introduction

Traumatic brain injury (TBI) is defined as an acute intracranial injury caused by external physical force. TBI is a leading cause of death and disability in the United States [1]. Although the mechanisms underlying TBI are under intense investigation, there is still no cure. The prognosis for recovery from TBI is dependent on the location, severity, and mechanism of the injury. Primary neurodegeneration caused by the acute initial impact inevitably triggers waves of secondary injury from inflammation [2–5] and initiates progressive neuronal demise in multiple regions of the brain [6–8]. These damaging sequelae can lead to behavioral deficits [8–11] and even psychosis [12–14]. The behavioral deficits from TBI involve dysfunction in sensorimotor abilities, memory, and cognition.

Apart from pharmacological approaches [15–19], recent advances in stem cell transplantation in non-TBI paradigms [20–24] have provided another novel approach towards the treatment of TBI. Coupled with the use of bioactive scaffolds to support extended survival and differentiation, stem cell transplantations have been successful in eliciting recovery from many injuries [25–27]. The functions of bioactive scaffolds are no longer limited to rendering physical support for stem cells. Some scaffolds can mitigate inflammatory responses when used *in vivo* [28] while providing a favorable environment for extended survival and differentiation of stem cells. In addition, stem cells at the injured sites continuously secrete neuroprotective protein factors [29–34] that promote the survival of surrounding cells. Scaffold-stem cell transplantation is therefore not only expected to prevent neuronal/tissue loss, but also to provide differentiated cells that integrate into and repair the damaged neural network.

In this study, we evaluated the therapeutic potential of urinary bladder matrix (UBM) loaded with neural stem cells (NSCs). These transplants were introduced into the rat brain following controlled cortical impact (CCI). We measured short and long term behavioral deficits induced by TBI. Transplantation of stem cells in the UBM scaffold significantly attenuated both motor and cognitive behavioral deficits. UBM alone was sufficient to confer short term protection of motor function. However, UBM with NSCs were required to elicit long term protection against memory and cognitive deficits. In sum, scaffold-stem cell transplantation is able to reduce neuron/tissue loss and attenuate behavioral deficits and white matter injury. Therefore, this approach holds promise for combating the primary and secondary changes elicited by TBI.

Material and Methods

Material

All the materials used in these experiments were obtained from Sigma-Aldrich (St. Louis, MI) unless stated otherwise.

Methods

Isolation and culture of neural stem cells—NSCs were isolated from 2 month old male C57BL/6j mice according to previously published methods [35]. Briefly, each isoflurane-anesthetized rat was decapitated and the brain was removed and placed in an ice-cold HBSS solution (Life Technologies, Grand Island, NY). The subventricular zone (SVZ) was carefully dissected and transferred into 0.25% trypsin. After incubation at room temperature for 30 min at 37°C, cells were harvested and pelleted by centrifugation and then re-suspended in proliferation medium (Stemcell Tech, Vancouver, Canada). Cell number was estimated by haemocytometer and 1×10^5 cells / well were plated into 24-well plates. After 24 hours, a complete medium changed was performed. Henceforth, medium was exchanged every 3 days. Typically, neurospheres appeared after 7 days and remained suspended. Neurospheres were collected by centrifugation (200×g, 5 min) for subsequent plating. Large neurospheres (>100μm) were dissociated into single cells about once every 10 days to facilitate their proliferation.

Animal model of traumatic brain injury—All animal experiments were approved by the Institutional Animal Care and Use Committee of Beijing Capital Medical University and performed in accordance with the NIH *Guide for the Care and Use of Laboratory Animals*. Efforts were made to minimize suffering and the number of animals used.

All animals were randomly assigned into experimental groups through the use of a lottery drawing. Three month old adult male Sprague-Dawley rats (280–320g) were housed under a 12-hour light/dark cycle in a temperature- and humidity-controlled animal facility. Rats were subjected to unilateral CCI as described previously with slight modifications [36]. General anesthesia was induced in a chamber with 4% isoflurane in oxygen. Animals were then fixed on a stereotaxic frame. Isoflurane was maintained at 1.5–2.5% during surgery. A right parietal craniotomy (3.0 mm lateral to the middle suture, diameter 5.4 mm) was made with a drill under aseptic conditions. CCI was produced using a pneumatically-driven cortical impact device (TBI 0310, Precision Systems and Instrumentation, Fairfax Station, VA) with a 5 mm diameter flat-tipped impactor that compressed the exposed dura mater and underlying brain to a depth of 3.2 mm for 0.5 s at 4.0 m/s velocity. Core body temperature was maintained at 36.5–37.5°C throughout the experiment. Sham controls were anesthetized and only subjected to right parietal craniotomy.

Preparation of UBM solution—UBM powder was obtained as previously described [37]. Briefly, porcine urinary bladders were harvested from 6-months-old pigs weighing around 108–118 kg (Thomas Meat Market, Saxonburg, PA) immediately following euthanasia. First, the excess connective tissue and residual urine were removed. The tunica serosa, tunica muscularis externa, tunica submucosa, and the majority of the tunica

muscularis mucosa were mechanically removed. The luminal surface was first soaked with 1.0 N saline to dissociate the urothelial cells of the tunica. The resulting biomaterial, which was composed of the basement membrane of the urothelial cells plus the subjacent lamina propria, was referred to as urinary bladder matrix (UBM). UBM sheets were placed in a solution containing 0.1% (v/v) peracetic acid, 4% (v/v) ethanol, and 95.9% (v/v) sterile water for 2 hours. To remove the peracetic acid residue, two 15-min washes with phosphate buffered saline (PBS, pH = 7.4) were performed, followed by another two 15-min washes with sterile water. The decellularized UBM sheets were then lyophilized using the Model 8–54 Bulk Freeze Dryer (FTS Systems, Inc., Stoneridge, N.Y.)). Enzymatic degradation products were generated as previously described [16]. Briefly, lyophilized scaffold materials were powdered using a Wiley mill through a 40 mesh screen. The powdered material was solubilized at a concentration of 10 mg/ml in a solution containing 1.0 mg/ml pepsin in 0.01 N HCl with a constant stir rate for 48h. The extracellular matrix digest solution was then frozen at −20°C until use in subsequent experiments. Enzymatic digestion was stopped by raising the pH of the solution to 7.4 using NaOH and diluting the solution to the desired concentration with PBS prior to further testing. In the present study, the material was diluted to a final concentration of a 5 mg/ml solution at 4°C. All solutions were kept at 4°C before and after being mixed together by vortex to prevent gelling. The mixed solution was centrifuged at 1000 rpm for 2 min to eliminate bubbles before injection.

Injection of UBM and UBM with NSCs into injured brain—At 24 hours following CCI injury, rats were anesthetized and placed in a stereotaxic frame. Core body temperature was monitored continuously by a rectal thermistor probe and maintained at 37 ± 0.5° C with a heating pad. The surgical site was reopened, and the burr hole was re-exposed. Through the burr hole, we infused four 2.5μl deposits of cell suspension in Dulbecco's PBS (Life technologies, Grand Island, NY) at a density of 0.5×10^5 NSCs per μL, or Dulbecco's PBS alone, UBM alone, or UBM containing NSCs (0.5×10^5 cells per μL) along the anterior-posterior axis of the cortex or the dorsal hippocampus just above the pyramidal neuron layers of CA3. Experimental groups thus consisted of vehicle (n = 10), NSCs alone (n = 10), UBM alone (n = 10), and UBM with NSCs (n = 10) following CCI or sham-operated controls (n = 6). The following coordinates were used: (1) anteroposterior (A-P), −0.5mm; mediolateral (M-L), +3.0mm; dorsoventral (D-V), −2.5mm; (2) A-P, −1.5mm; M-L, +3.0mm; D-V, −2.5mm; (3) A-P, −2.5mm; M-L, +3.0mm; D-V, −2.0mm; (4) A-P, −3.5mm; M-L, +2.0mm; D-V, −3.0mm. The injections were performed using a 10μl Hamilton syringe controlled by a Micro 4 Micro-syringe Pump Controller (World Precision Instruments, Sarasota, FL). Each injection lasted for 5 minutes and was followed by 15 minutes of rest before needle withdrawal. After 28 days of neurobehavioral testing, rats were sacrificed by perfusion and brains were prepared for tissue analyses as described below.

Foot fault tests—Sensorimotor function of affected rat limbs after CCI was evaluated by the forelimb and hindlimb foot fault tests as described [38]. These tests were performed by two investigators who were blinded to experimental group. Animals were placed on an elevated horizontal ladder with a regular arrangement of rungs at 2 cm intervals. Before surgery, the rats were trained for 3 consecutive days to obtain the baseline score of the foot fault test. The forelimb and hindlimb foot fault test was performed at day 3, 5, 7, 14, and 28

after CCI. Rats were trained and tested three times daily. Analysis was performed on videotapes, and quantitative evaluation was made using a 7-category scale [38]. Scores were determined as the average of three trials.

Morris water maze test—The Morris water maze test was performed to detect spatial learning and memory impairments daily from day 23–27 post-CCI [39] by two investigators who were blinded to experimental group. The water maze was a black circular pool positioned in the middle of a room with various distal visual stimuli as spatial cues. The tank was filled with 20–22 °C water to a depth 0.3 m. On the first 4 consecutive days (day 23–26 after CCI), the rats were tested for the acquisition of the reference memory task. A stable circular platform was submerged 2 cm below the water surface. Each rat was placed in the pool at different starting positions for five consequent trials every day with a 10 second interval. Animals were given 60 seconds to locate the hidden platform. If the hidden platform was not found within the given time, the rats were manually guided to it and remained on the platform for 10 seconds. The escape latency of every trial was recorded and the average of five trials per day was used for analysis. At day 27 post-CCI, a probe test was performed with the escape platform removed. Rats were released into the pool from the point most distal to the target quadrant in which the platform was previously located. The time spent by the rat in the target quadrant searching for the platform was recorded for analysis.

Cresyl violet staining and lesion volume measurement—Cresyl violet staining was performed to calculate lesion volumes. Brains were sliced at 30 μm on a sliding microtome. The free-floating serial coronal sections were mounted onto color frost/plus slides (Fisher Scientific, Pittsburgh, PA). After air-drying, sections were stained with cresyl violet. For lesion volume measurements, six brain sections from each rat were traced by a microcomputer imaging device (MCID; Imaging Research, St. Catharine's, Ontario, Canada). The lesion area on each section (ΣAi) was calculated (i.e., the intact area of the ipsilateral hemisphere is subtracted from the area of the contralateral hemisphere) by an investigator blinded to the study groups, and the lesion volume was obtained by multiplying lesion areas with the distance between the sections. These volumes were summed to get a final volume for the rostrocaudal extent of the lesion.

Stereological Cell Counting of CA3 Neurons

After Nissl staining at 28 days after CCI, viable CA3 neurons were quantified stereologically by an investigator blinded to the experimental groups as previously described [40]. Image of the CA3 subfield was captured with a color CCD to camera, with 50×50-μm grid squares over the region of interest, and with 100 to 150 cells that were counted in a given structure for the optical dissector method to estimate the total number. A dissector was defined as the number of neurons within the 25×25×25-μm box. On average, 9 dissectors per section yielded the desired number of counted neurons throughout the dorsal hippocampal CA3, and the number of dissectors was maintained at a constant ratio from section to section. The rostro-caudal length of the CA3 was 1 mm (from bregma −0.94 mm to bregma −1.94 mm), which was obtained by multiplying section thickness by the number of sections (25 sections). Every fifth section was quantified. The total number of neurons was calculated

using the optical dissector, equal to the quotient of the total number of neurons counted and the product of the fractions for sampling section frequency (SSF) or fraction of sections counted, the area section frequency (ASF) or sampling area/area between the dissectors, and the thickness section frequency (TSF) or the dissector depth/section thickness, for n0Σ neurons counted×1/SSF×1/ASF×1/TSF). For our study, SSF01/4 sections, ASF025×25 μM/50×50 μM, and TSF025 μM/40 μM.

Immunofluorescence staining—For immunofluorescent staining, sections through the brain regions of interest were first blocked with 10% goat serum/PBS solution for 1 hour and then incubated with mouse anti-SMI32 antibody (non-phosphorylated neurofilament H monoclonal, 1:250, Covance, Princeton, NJ, USA) and rabbit anti-myelin basic protein 1 (MBP-1) antibody (1:250, Millipore, Billerica, MA, USA) for 1 hour at 37°C each and then at 4°C overnight. On the following day, following three washes in PBS, sections were incubated in a mixture of anti-mouse secondary antibody conjugated with DyLight™ 594 (Jackson ImmunoResearch Laboratories) and anti-rabbit secondary antibody conjugated with DyLight™ 488 (Jackson ImmunoResearch Laboratories, West Grove, PA, USA) for 1 hour at 37°C. Subsequently, the sections were placed on glass slides and coversliped with VECTASHIELD mounting medium containing DAPI (Vector Laboratories Inc., Burlingame, CA) prior to confocal fluorescence microscopy (FV1000, Olympus, Japan).

Statistical analyses—All values are presented as mean ± standard error. Data with two groups were analyzed with the Student's *t*-test (non-directional), and data with repeated groups were analyzed with one-way ANOVA and the Bonferroni/Dunn tests for *post hoc* comparisons. The Pearson product linear regression analysis was used to correlate the number of CA3 neurons with spatial memory and to correlate the SMI32/MBP immunofluorescence ratio with spatial memory. Differences were considered statistically significant at $p<0.05$.

Results

The success of NSC transplantation can be enhanced in the presence of an environment that is favorable for their extended survival and subsequent integration into the neural network. Previous studies have shown a significant attenuation in TBI induced neuronal loss by fetal neural tissue grafts [41]. These findings also reflect the importance of matrix support of cells and cell-cell interactions *in vivo*. In the present study, we assessed the efficacy of porcine UBM to support NSC viability and differentiation *in vitro* and *in vivo*. We also evaluated the therapeutic potential of NSC/UBM transplantation against a rat model of TBI.

NSCs in culture undergo differentiation to various lineages

NSCs were isolated from the SVZ of male 2 month old mice. After dissociation from the collagen matrix, NSCs were seeded in culture plates. After 10 days, the surviving NSCs have a high propensity to form spheres. Neural spheres reaching 100–200μm were further dissociated mechanically to smaller spheres so that each cell could contact proliferation medium prior to plating on culture plates. The purity of the NSC culture was ascertained via

immunostaining for nestin (Figure 1A). Typically, only NSC cultures of 90% or greater purity were used in subsequent experiments.

Next, the pluripotency of the NSC cultures was ascertained. The proliferation medium used for NSC cultures was switched to differentiation medium. After 7 days, the NSC spheres had flattened and attached onto the substratum. Neurite extensions for a subset of cells were observed. The lineages of the cell populations derived from NSC were determined by immunostaining for phenotypic markers of neurons (β-Tubulin III, Figure 1B, panel A green signal), astrocytes (GFAP, Figure 1B, panel A red signal), and oligodendrocytes (O4, Figure 1B, panel B green signal). All three markers were present and indicated the differentiation of NSC to neuronal, astrocytic, and oligodendrocytic lineages. In sum, the NSCs isolated and purified from the SVZ retained their pluripotency and were suitable for grafting.

UBM stabilizes NSCs in the undifferentiated state better than matrigel

Thus far, collagen and matrigel (derived from tumor cells) matrices have been shown to support extended growth of stem cells [42–47]. However, the lack of bioactive factors for the former and the tumor inducing potential for the latter have limited their therapeutic use. Recently, a new extracellular matrix derived from porcine urinary bladder was successfully used in tissue engineering [48–50]. In this study, we evaluated UBM as a viable matrix to support NSC proliferation for an extended duration, using matrigel for comparison. As expected, UBM was able to support the proliferation of NSCs at high rates (>80% viability, 7 days) with an average doubling time of 47.2 hours (Figure 1C, panel C). After 2 weeks, NSCs in UBM remained undifferentiated whereas NSCs in matrigel underwent spontaneous and progressive differentiation after 24 hours (Figure 1C, panel A and B), indicating that UBM provided a more stable environment for NSCs to remain undifferentiated.

When UBM containing NSCs was exposed to differentiation medium for 7 days, the pluripotent stem cells underwent differentiation to neuronal, astrocytic, and oligodendrocytic lineages as visualized by immunostaining for their respective markers (Figure 1C, panel D–F). To compare UBM with matrigel, we harvested NSCs grown in UBM or matrigel after 2 weeks in differentiation medium to ascertain the levels of lineage markers by Western blot analysis. For both cultures, the levels of Tuj1 and GFAP were comparable (Figure 1C, panel G) suggesting equivalent support from UBM and matrigel for NSC proliferation and differentiation.

UBM facilitates NSC survival and proliferation *in vivo* after TBI

After ascertaining that NSCs were able to proliferate and differentiate in UBM, we examined the ability of UBM to support NSC proliferation *in vivo*, especially after injury from CCI. Male rats were subjected to CCI and 24 hours later, the hippocampus was infused with BrdU-labeled NSCs, NSC-loaded UBM, UBM without NSC, or PBS. Three days post-injection, the survivability and proliferation of NSCs at the injection sites were examined by immunostaining for nestin and BrdU, respectively (Figure 2A). Rats injected with BrdU-labeled NSCs without UBM showed weak BrdU signal around the injection sites (Figure 2A, panel A). However, injections with BrdU-labeled NSCs with UBM showed a significant number of BrdU labeled NSCs still present around the injection sites (Figure 2A, panel B).

Staining with nestin showed that, in the absence of UBM, there were few NSCs around the injection sites and little penetrance into brain parenchyma (Figure 2A, panel C). In contrast, NSCs in UBM showed a significantly higher number of NSCs around the injection sites and a wider distribution (Figure 2A, panel D).

At 7 days post-injection, the proliferation and differentiation of NSCs in the injured cortex were also examined by immunostaining for nestin and the neuronal phenotypic marker MAP-2. Rats injected with NSCs without UBM showed very few NSCs (red) and a significant loss of neurites as reflected by the decrease in MAP-2 signal (green) 7 days post-injection at or around the injury (Figure 2B, panel A–C). On the other hand, rats injected with NSC in UBM showed a strong nestin signal, suggesting a healthy population of NSCs in the injured cortex. In addition, robust MAP-2 staining revealed the presence of abundant neurites in this group (Figure 2B, panel D–F). The inset frames of Figure 2B, panels D–F are magnified for detailed examination of the potential differentiation of exogenous NSC in the injured cortex (Figure 2B, panel G–I). In these images, the presence of overlapping signal (red and green) and neuritic extensions suggest that these cells were undergoing differentiation. In sum, the results indicate that UBM is able to support extended survival of NSC and permits their differentiation.

NSC-UBM attenuates tissue loss and mitigates motor function impairments

In view of the attenuation of neurite loss (reflected by MAP-2 staining) around the injection sites from NSC transplantation in the presence of UBM, we investigated the impact of NSCs and UBM on CCI-induced behavioral impairments. For this, NSC-loaded UBM, UBM alone, NSCs in PBS, or PBS alone were stereotaxically injected along the rostrocaudal axis of the cortex or the dorsal hippocampus just above the pyramidal neuron layers of CA3 at 24 hours after CCI. An additional group of sham animals were not subjected to CCI. To assess changes in motor function, rats from each group were randomly selected to perform forelimb and hindlimb foot-fault tests before CCI and at 3-, 5-, 7-, 14, 21-, and 28 days post-CCI. Performances on these tests are presented in Figure 3A–D. As expected, there was a sharp decrease in scores for the forelimb and hindlimb performance 3 days post-CCI, followed by a gradual increase in performance scores as the animals recovered sensorimotor function. This pattern was evident in the rats receiving CCI + vehicle. Introducing NSCs alone did not significantly alter the forelimb and hindlimb performance scores relative to the group receiving CCI + vehicle (Figure 3A and B). On the other hand, rats receiving UBM alone or UBM seeded with NSCs experienced less of a drop in forelimb and hindlimb performance scores 3 days post-CCI. This significant improvement in performance was maintained for the duration of both tests. Surprisingly, there was no significant difference in performance scores for rats receiving UBM alone and UBM seeded with NSCs for the hindlimb test (Figure 3D). As for the forelimb test, rats receiving UBM seeded with NSCs performed better than those receiving UBM alone at 14 days post-CCI.

To compare tissue loss, serial coronal brain sections harvested at 28 days post-CCI were stained with cresyl violet. The lesion size was largest in rats receiving CCI + vehicle and CCI + NSC and significantly smaller lesion sizes were observed in rats receiving either UBM alone or UBM loaded with NSCs (Figure 3E). There was no significant difference in

tissue loss between rats receiving CCI + UBM alone and CCI + UBM-NSC (Figure 3F). In sum, these results suggested that UBM alone is sufficient to confer short term protection against motor function impairments and tissue loss.

NSC-UBM enhances viable neurons in CA3 and decreases memory and cognitive deficits

Next, we measured the impact of UBM and NSCs on CCI-induced memory and cognitive deficits by using the Morris water maze test. Randomly chosen rats from the same treatment groups as above were subjected to the water maze test daily from 23- to 26-days post-CCI. Rats receiving CCI + vehicle had the highest latency time before identifying the platform (Figure 4A) and spent the shortest amount of time in the same quadrant as the submerged platform (Figure 4B) indicating that these rats experienced the greatest memory and cognitive deficit due to CCI. Unlike the improvement in motor function, rats receiving CCI + UBM alone did not perform significantly better than those receiving CCI + vehicle in the Morris water maze. However, rats receiving CCI + UBM-NSC performed significantly better than those receiving CCI + vehicle or CCI + UBM alone. In sum, these results indicate that only rats receiving CCI + UBM-NSC exhibited a decrease in memory and cognitive impairments. In other words, long term protection is only possible with the use of UBM seeded with NSCs.

The number of viable neurons in the CA3 region of the hippocampus of the ipsilateral hemisphere was counted to determine neuroprotection. Rats receiving CCI + UBM-NSC had a significantly higher percentage of viable neurons in this region than those receiving CCI + UBM alone, CCI + NSC and CCI + vehicle (Figure 4C). In addition, there was a direct correlation between the percentage of viable neurons and the amount of time spent in the same quadrant as the target platform (Figure 4D) suggesting that the preservation of viable neurons in the CA3 region of the hippocampus may have contributed to the improvement in memory and cognitive ability.

Treatment with UBM-NSC decreases white matter injury

Similar to ischemic injury, CCI also induces white matter injury, which may contribute to the loss in memory and cognitive ability. White matter injury can be assessed by staining for SMI32 and MBP in the cortex and striatum around the CCI lesion, as indicated in Figure 5C. In the striatum (Figure 5A) and cortex (Figure 5B), there was a sharp increase in SMI32 in rats receiving CCI + vehicle compared to sham. Concomitantly, a decrease in MBP staining was observed in both regions in rats receiving CCI + vehicle. In contrast, rats receiving CCI + UBM-NSC showed significantly weaker staining for SM132 and more robust staining for MBP in both regions compared to the CCI + vehicle group.

SMI32 and MBP staining intensities were averaged from a minimum of 6 images of the striatum and cortex, thereby enabling the determination of the SMI32/MBP ratio. In the striatum, the relative SMI32/MBP ratio was substantially higher in rats receiving CCI + vehicle than sham, indicating increased white matter injury. A significantly lower SMI32/MBP ratio was observed in rats receiving CCI + UBM alone than those receiving CCI + vehicle, suggesting that UBM alone can attenuate CCI-induced white matter injury. The presence of NSCs in UBM reduced the SMI32/MBP ratio even further, suggesting that

the inclusion of NSCs can significantly ameliorate white matter injury (Figure 5D). A similar trend in the SMI32/MBP ratio across treatment groups was observed in the cortex. However, the difference between UBM with NSC and UBM alone was not statistically significant (Figure 5E).

Finally, the SMI32/MBP ratio was found to be inversely proportional to time spent in the same quadrant as the target platform in the Morris water maze test (Figure 5F) suggesting that a decrease in white matter injury is associated with improved memory and cognition. Thus, the impact of UBM alone and UBM with NSCs on white matter injury may improve memory and cognition.

Discussion

The complex primary and secondary pathologies of TBI have made a cure for this disabling disease elusive. The prognosis for a patient with severe TBI can therefore be grim. The primary and secondary waves of injury after TBI lead to short and long term behavioral impairments due to neurodegeneration and white matter injury. In this study, we evaluated the efficacy of transplantation of NSCs coupled to a three-dimensional bioactive matrix scaffold made from urinary bladder. We measured whether this transplantation strategy attenuated injury induced by TBI. NSC and UBM transplantation elicited significant short and long-term protection against behavioral deficits, neurodegeneration, and white matter injury. Hence, transplantation of cells in a bioactive matrix provides a promising novel therapeutic strategy for TBI as well as other neurological disorders.

In this study, the decision to use UBM as the bioactive scaffold to support NSC proliferation, differentiation and migration was based on previous studies in our and other laboratories [48, 49, 51]. UBM and its derivatives have been used successfully as extracellular matrix in external tissue construction [48–50] and to support repair [25–27]. First, our UBM characterization studies revealed an excellent biocompatibility with the brain since it did not elicit inflammatory responses greater than vehicle over the course of 3–4 weeks (data not shown). This property was originally demonstrated when UBM was used in conjunction with polypropylene mesh in pelvic surgery [28]. In addition, we have found that implantation of UBM did not elicit reactive astrocytosis either (data not shown). The lack of an astrocytic scar at the injection site suggests the rapid degradation of UBM. Furthermore, UBM supports the proliferation and differentiation of mesenchymal osteoprogenitors [51] and NSCs (Figure 1, 2). We conclude that UBM provides a suitable microenvironment for enhanced cell viability.

Post-injury introduction of UBM alone and UBM seeded with NSCs elicited significant and comparable short-term protection against tissue loss and motor deficits (Figure 3). It may seem surprising that NSCs did not further mitigate motor impairments. This outcome may suggest that the extent of the short term injury is only sensitive to the UBM-influenced microenvironment at and around the lesion. Degeneration and inflammation at the lesion site are likely to be self- and mutually propelling [52–54]. Primary degeneration may elicit inflammation, which can trigger chronic neurodegeneration and the onset of clinical symptoms. The anti-inflammatory properties of UBM may provide a more protective

microenvironment and mitigate secondary neurodegeneration [28]. Typically, the cumulative neuronal loss in the first 3 days post injury dictates the onset of motor deficits. It seems unlikely that NSCs would complete their differentiation and integrate themselves into the existing neural network within this short timeframe. This may account for the lack of significant difference in short term protection between UBM alone and UBM with NSC.

On the other hand, only UBM containing NSCs elicited significant long term protection against impairments in memory and cognition. In other words, comparable long term behavioral deficits were observed in rats injected with UBM alone or vehicle. This result suggests that UBM alone did not provide a sufficiently favorable microenvironment to elicit long term protection. This failure may be due to the rapid degradation (14 days) of UBM *in vivo* [28]. Upon UBM degradation, the favorable microenvironment may be lost in the CA3 region of the hippocampus (Figure 4C). However, when NSCs are injected with UBM and differentiate, this could replace lost neurons for the long haul [55]. In addition, NSCs are known to elicit a bystander effect [56], where they secrete neuroprotective molecules that favor cell survival [29–34] and tissue repair [57], perhaps even after UBM is degraded. One might also infer from this result that hippocampal demise is a late event triggered by inflammation, and that UBM cannot prevent late neurodegenerative events.

In contrast to the hippocampal viability data, the attenuation of white matter injury by UBM alone and UBM with NSCs may result from a combination of anti-inflammatory effects of UBM and protective effects of NSCs. The protection of white matter injury in both groups suggests that this type of injury may occur at both early and late stages after TBI.

In summary, the combined use of UBM and NSCs is a viable strategy to confer both short and long term protection against neuronal and tissue loss as well as motor and cognitive deficits. Notably, this strategy is protective even if the intervention follows the neurological injury, making it more relevant to the clinical situation. Thus, NSCs in a bioactive UBM scaffold hold promise as a novel therapeutic strategy for TBI and other neurological disorders.

Conclusion

The present study demonstrates that the combination of UBM-NSCs is a viable strategy to protect against neuronal loss and to reduce lesion volume, white matter injury, and motor and cognitive dysfunction even when administered after TBI. Specifically, UBM alone can confer short term protection against motor impairments. However, the presence of NSCs in this matrix is mandatory for long term protection of memory and cognition. Thus, stem cells housed within a 3-dimensional matrix are an excellent strategy to achieve functional recovery after TBI.

Acknowledgments

This work was supported by the Department of Defense Concept grant (to J.C. and X.T.C,), the National Institutes of Health Grants (NS36736, NS43802, and NS45048 to J.C), and National Science Foundation (DMR-0748001 to X.T.C.). L.C. was supported by grants from the National Natural Science Foundation of China (Grant # 81272804 and 30970939), the Key Project of Chinese Ministry of Education (Grant # 210003), and the High Level Talent Fund from the Beijing Healthcare System (Grant # 2011-3-093). X.J. was supported by grants from the National

Natural Science Foundation of China (Grant # 30870854 and 81171241) and the National Basic Research Program of China (973 Program) (Grant # 2011CB707804).

List of Abbreviation

NSC	Neural Stem Cell
UBM	Urinary Bladder Matrix
TBI	Traumatic Brain Injury
CCI	Controlled Cortical Impact

References

1. Coronado VG, Xu L, Basavaraju SV, McGuire LC, Wald MM, Faul MD, Guzman BR, Hemphill JD. Surveillance for traumatic brain injury-related deaths--United States, 1997–2007. MMWR Surveill Summ. 2011; 60(5):1–32. [PubMed: 21544045]
2. Cao T, Thomas TC, Ziebell JM, Pauly JR, Lifshitz J. Morphological and genetic activation of microglia after diffuse traumatic brain injury in the rat. Neuroscience. 2012; 225:65–75. [PubMed: 22960311]
3. Kumar A, Loane DJ. Neuroinflammation after traumatic brain injury: Opportunities for therapeutic intervention. Brain, behavior, and immunity. 2012; 26(8):1191–1201.
4. Lewis M, Ghassemi P, Hibbeln J. Therapeutic use of omega-3 fatty acids in severe head trauma. The American journal of emergency medicine. 2012
5. Ziebell JM, Morganti-Kossmann MC. Involvement of pro- and anti-inflammatory cytokines and chemokines in the pathophysiology of traumatic brain injury. Neurotherapeutics : the journal of the American Society for Experimental NeuroTherapeutics. 2010; 7(1):22–30. [PubMed: 20129494]
6. Han SH, Chung SY. Marked hippocampal neuronal damage without motor deficits after mild concussive-like brain injury in apolipoprotein E-deficient mice. Annals of the New York Academy of Sciences. 2000; 903:357–365. [PubMed: 10818526]
7. Lifshitz J, Lisembee AM. Neurodegeneration in the somatosensory cortex after experimental diffuse brain injury. Brain structure & function. 2012; 217(1):49–61. [PubMed: 21597967]
8. Wang H, Lynch JR, Song P, Yang HJ, Yates RB, Mace B, Warner DS, Guyton JR, Laskowitz DT. Simvastatin and atorvastatin improve behavioral outcome, reduce hippocampal degeneration, and improve cerebral blood flow after experimental traumatic brain injury. Experimental neurology. 2007; 206(1):59–69. [PubMed: 17521631]
9. Ding Y, Yao B, Lai Q, McAllister JP. Impaired motor learning and diffuse axonal damage in motor and visual systems of the rat following traumatic brain injury. Neurological research. 2001; 23(2–3):193–202. [PubMed: 11320599]
10. Huh JW, Widing AG, Raghupathi R. Midline brain injury in the immature rat induces sustained cognitive deficits, bihemispheric axonal injury and neurodegeneration. Experimental neurology. 2008; 213(1):84–92. [PubMed: 18599043]
11. Piot-Grosjean O, Wahl F, Gobbo O, Stutzmann JM. Assessment of sensorimotor and cognitive deficits induced by a moderate traumatic injury in the right parietal cortex of the rat. Neurobiology of disease. 2001; 8(6):1082–1093. [PubMed: 11741403]
12. Fujii D, Fujii DC. Psychotic disorder due to traumatic brain injury: analysis of case studies in the literature. The Journal of neuropsychiatry and clinical neurosciences. 2012; 24(3):278–289. [PubMed: 23037642]
13. Reeves RR, Panguluri RL. Neuropsychiatric complications of traumatic brain injury. Journal of psychosocial nursing and mental health services. 2011; 49(3):42–50. [PubMed: 21323264]
14. Guerreiro DF, Navarro R, Silva M, Carvalho M, Gois C. Psychosis secondary to traumatic brain injury. Brain injury : [BI]. 2009; 23(4):358–361.
15. Methylphenidate improves cognitive function during rehabilitation after TBI. Nature clinical practice Neurology. 2009; 5(3):125.

16. Sawyer E, Mauro LS, Ohlinger MJ. Amantadine enhancement of arousal and cognition after traumatic brain injury. The Annals of pharmacotherapy. 2008; 42(2):247–252. [PubMed: 18212258]

17. Shein NA, Grigoriadis N, Alexandrovich AG, Simeonidou C, Lourbopoulos A, Polyzoidou E, Trembovler V, Mascagni P, Dinarello CA, Shohami E. Histone deacetylase inhibitor ITF2357 is neuroprotective, improves functional recovery, and induces glial apoptosis following experimental traumatic brain injury. FASEB journal : official publication of the Federation of American Societies for Experimental Biology. 2009; 23(12):4266–4275. [PubMed: 19723705]

18. Trovato M, Slomine B, Pidcock F, Christensen J. The efficacy of donepezil hydrochloride on memory functioning in three adolescents with severe traumatic brain injury. Brain injury : [BI]. 2006; 20(3):339–343.

19. Wheaton P, Mathias JL, Vink R. Impact of pharmacological treatments on cognitive and behavioral outcome in the postacute stages of adult traumatic brain injury: a meta-analysis. Journal of clinical psychopharmacology. 2011; 31(6):745–757. [PubMed: 22020351]

20. Zhao YH, Guan Y, Wu WK. Potential advantages of a combination of chinese medicine and bone marrow mesenchymal stem cell transplantation for removing blood stasis and stimulating neogenesis during ischemic stroke treatment. Journal of traditional Chinese medicine = Chung i tsa chih ying wen pan / sponsored by All-China Association of Traditional Chinese Medicine, Academy of Traditional Chinese Medicine. 2012; 32(2):289–292.

21. Snyder EY, Teng YD. Stem cells and spinal cord repair. The New England journal of medicine. 2012; 366(20):1940–1942. [PubMed: 22591301]

22. Liew A, O'Brien T. Therapeutic potential for mesenchymal stem cell transplantation in critical limb ischemia. Stem cell research & therapy. 2012; 3(4):28. [PubMed: 22846185]

23. Larijani B, Esfahani EN, Amini P, Nikbin B, Alimoghaddam K, Amiri S, Malekzadeh R, Yazdi NM, Ghodsi M, Dowlati Y, et al. Stem cell therapy in treatment of different diseases. Acta medica Iranica. 2012; 50(2):79–96. [PubMed: 22359076]

24. Hodgetts SI, Simmons PJ, Plant GW. Human Mesenchymal Precursor Cells (Stro-1(+)) from Spinal Cord Injury Patients Improve Functional Recovery and Tissue Sparing in an Acute Spinal Cord Injury Rat Model. Cell transplantation. 2012

25. Badylak S, Obermiller J, Geddes L, Matheny R. Extracellular matrix for myocardial repair. The heart surgery forum. 2003; 6(2):E20–26. [PubMed: 12716647]

26. Gilbert TW, Nieponice A, Spievack AR, Holcomb J, Gilbert S, Badylak SF. Repair of the thoracic wall with an extracellular matrix scaffold in a canine model. The Journal of surgical research. 2008; 147(1):61–67. [PubMed: 17950323]

27. Shah U, Bien H, Entcheva E. Microtopographical effects of natural scaffolding on cardiomyocyte function and arrhythmogenesis. Acta biomaterialia. 2010; 6(8):3029–3034. [PubMed: 20197129]

28. Liu L, Deng L, Wang Y, Ge L, Chen Y, Liang Z. Porcine urinary bladder matrix-polypropylene mesh: a novel scaffold material reduces immunorejection in rat pelvic surgery. International urogynecology journal. 2012; 23(9):1271–1278. [PubMed: 22538554]

29. Campos LS, Decker L, Taylor V, Skarnes W. Notch, epidermal growth factor receptor, and beta1-integrin pathways are coordinated in neural stem cells. The Journal of biological chemistry. 2006; 281(8):5300–5309. [PubMed: 16332675]

30. Campos LS, Leone DP, Relvas JB, Brakebusch C, Fassler R, Suter U, ffrench-Constant C. Beta1 integrins activate a MAPK signalling pathway in neural stem cells that contributes to their maintenance. Development. 2004; 131(14):3433–3444. [PubMed: 15226259]

31. Ji JF, He BP, Dheen ST, Tay SS. Expression of chemokine receptors CXCR4, CCR2, CCR5 and CX3CR1 in neural progenitor cells isolated from the subventricular zone of the adult rat brain. Neuroscience letters. 2004; 355(3):236–240. [PubMed: 14732474]

32. Ji JF, He BP, Dheen ST, Tay SS. Interactions of chemokines and chemokine receptors mediate the migration of mesenchymal stem cells to the impaired site in the brain after hypoglossal nerve injury. Stem Cells. 2004; 22(3):415–427. [PubMed: 15153618]

33. Pluchino S, Quattrini A, Brambilla E, Gritti A, Salani G, Dina G, Galli R, Del Carro U, Amadio S, Bergami A, et al. Injection of adult neurospheres induces recovery in a chronic model of multiple sclerosis. Nature. 2003; 422(6933):688–694. [PubMed: 12700753]

34. Pluchino S, Zanotti L, Rossi B, Brambilla E, Ottoboni L, Salani G, Martinello M, Cattalini A, Bergami A, Furlan R, et al. Neurosphere-derived multipotent precursors promote neuroprotection by an immunomodulatory mechanism. Nature. 2005; 436(7048):266–271. [PubMed: 16015332]
35. Iosif RE, Ahlenius H, Ekdahl CT, Darsalia V, Thored P, Jovinge S, Kokaia Z, Lindvall O. Suppression of stroke-induced progenitor proliferation in adult subventricular zone by tumor necrosis factor receptor 1. Journal of cerebral blood flow and metabolism : official journal of the International Society of Cerebral Blood Flow and Metabolism. 2008; 28(9):1574–1587.
36. Gilmer LK, Roberts KN, Joy K, Sullivan PG, Scheff SW. Early mitochondrial dysfunction after cortical contusion injury. Journal of neurotrauma. 2009; 26(8):1271–1280. [PubMed: 19637966]
37. Freytes DO, Martin J, Velankar SS, Lee AS, Badylak SF. Preparation and rheological characterization of a gel form of the porcine urinary bladder matrix. Biomaterials. 2008; 29(11): 1630–1637. [PubMed: 18201760]
38. Metz GA, Whishaw IQ. Cortical and subcortical lesions impair skilled walking in the ladder rung walking test: a new task to evaluate fore- and hindlimb stepping, placing, and co-ordination. Journal of neuroscience methods. 2002; 115(2):169–179. [PubMed: 11992668]
39. Vorhees CV, Williams MT. Morris water maze: procedures for assessing spatial and related forms of learning and memory. Nature protocols. 2006; 1(2):848–858.
40. Wang G, Jiang X, Pu X, Zhang W, An C, Hu X, Liou AKF, Leak RK, Gao Y, Chen J. Scriptaid, a novel histone deacetylase inhibitor, protects against traumatic brain injury via modulation of PTEN and AKT pathway. Neurotherapeutics : the journal of the American Society for Experimental NeuroTherapeutics. 2012 in press.
41. Soares HD, Sinson GP, McIntosh TK. Fetal hippocampal transplants attenuate CA3 pyramidal cell death resulting from fluid percussion brain injury in the rat. Journal of neurotrauma. 1995; 12(6): 1059–1067. [PubMed: 8742134]
42. Dai W, Hale SL, Kay GL, Jyrala AJ, Kloner RA. Delivering stem cells to the heart in a collagen matrix reduces relocation of cells to other organs as assessed by nanoparticle technology. Regenerative medicine. 2009; 4(3):387–395. [PubMed: 19438314]
43. Jin K, Mao X, Xie L, Galvan V, Lai B, Wang Y, Gorostiza O, Wang X, Greenberg DA. Transplantation of human neural precursor cells in Matrigel scaffolding improves outcome from focal cerebral ischemia after delayed postischemic treatment in rats. Journal of cerebral blood flow and metabolism : official journal of the International Society of Cerebral Blood Flow and Metabolism. 2010; 30(3):534–544.
44. Kohen NT, Little LE, Healy KE. Characterization of Matrigel interfaces during defined human embryonic stem cell culture. Biointerphases. 2009; 4(4)::69–79. [PubMed: 20408727]
45. Kouris NA, Squirrell JM, Jung JP, Pehlke CA, Hacker T, Eliceiri KW, Ogle BM. A nondenatured, noncrosslinked collagen matrix to deliver stem cells to the heart. Regenerative medicine. 2011; 6(5):569–582. [PubMed: 21916593]
46. Mauney J, Olsen BR, Volloch V. Matrix remodeling as stem cell recruitment event: a novel in vitro model for homing of human bone marrow stromal cells to the site of injury shows crucial role of extracellular collagen matrix. Matrix biology : journal of the International Society for Matrix Biology. 2010; 29(8):657–663. [PubMed: 20828613]
47. Uemura M, Refaat MM, Shinoyama M, Hayashi H, Hashimoto N, Takahashi J. Matrigel supports survival and neuronal differentiation of grafted embryonic stem cell-derived neural precursor cells. Journal of neuroscience research. 2010; 88(3):542–551. [PubMed: 19774667]
48. Boruch AV, Nieponice A, Qureshi IR, Gilbert TW, Badylak SF. Constructive remodeling of biologic scaffolds is dependent on early exposure to physiologic bladder filling in a canine partial cystectomy model. The Journal of surgical research. 2010; 161(2):217–225. [PubMed: 19577253]
49. Davis NF, Callanan A, McGuire BB, Flood HD, McGloughlin TM. Evaluation of viability and proliferative activity of human urothelial cells cultured onto xenogenic tissue-engineered extracellular matrices. Urology. 2011; 77(4):1007, e1001–1007. [PubMed: 21256541]
50. Rosario DJ, Reilly GC, Ali Salah E, Glover M, Bullock AJ, Macneil S. Decellularization and sterilization of porcine urinary bladder matrix for tissue engineering in the lower urinary tract. Regenerative medicine. 2008; 3(2):145–156. [PubMed: 18307398]

51. Penolazzi L, Mazzitelli S, Vecchiatini R, Torreggiani E, Lambertini E, Johnson S, Badylak SF, Piva R, Nastruzzi C. Human mesenchymal stem cells seeded on extracellular matrix-scaffold: viability and osteogenic potential. Journal of cellular physiology. 2012; 227(2):857–866. [PubMed: 21830215]

52. Martino G. How the brain repairs itself: new therapeutic strategies in inflammatory and degenerative CNS disorders. Lancet neurology. 2004; 3(6):372–378. [PubMed: 15157853]

53. Martino G, Adorini L, Rieckmann P, Hillert J, Kallmann B, Comi G, Filippi M. Inflammation in multiple sclerosis: the good, the bad, and the complex. Lancet neurology. 2002; 1(8):499–509. [PubMed: 12849335]

54. Martino G, Pluchino S, Bonfanti L, Schwartz M. Brain regeneration in physiology and pathology: the immune signature driving therapeutic plasticity of neural stem cells. Physiological reviews. 2011; 91(4):1281–1304. [PubMed: 22013212]

55. Goldman S. Stem and progenitor cell-based therapy of the human central nervous system. Nature biotechnology. 2005; 23(7):862–871.

56. De Feo D, Merlini A, Laterza C, Martino G. Neural stem cell transplantation in central nervous system disorders: from cell replacement to neuroprotection. Current opinion in neurology. 2012; 25(3):322–333. [PubMed: 22547103]

57. Martino G, Pluchino S. The therapeutic potential of neural stem cells. Nature reviews Neuroscience. 2006; 7(5):395–406.

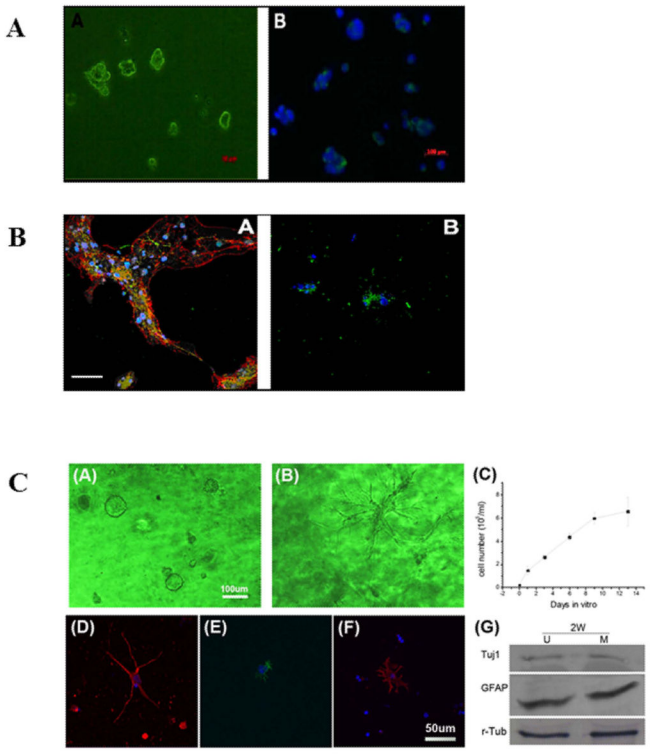

Figure 1. The bioactive scaffold UBM effectively supports the proliferation and differentiation of neural stem cells (NSCs)

(A) NSCs grown in culture. Representative images showing the cells after passage 6. NSCs were positive for nestin, an intermediate filament commonly found in neural precursors (panel A, green). Nuclei were stained with DAPI (panel B, blue); (B) Differentiated stem cells grown in culture. Representative confocal immunofluorescent images showing triple labeled differentiated NSCs after 7 days in differentiation medium (panel A); the fluorescent signal corresponds to nuclei (blue), GFAP (red), and β-tubulin-III (green). Representative confocal immunofluorescent images showing double labeled differentiated NSCs under the same treatment conditions (panel B); the fluorescent signal corresponds to nuclei (blue) and oligodendrocytic O4 (green). Scale bar: 100μm; (C) NSCs cultured in UBM (panel A) or matrigel (panel B) undergoing proliferation on day 9. UBM is better at maintaining NSCs in their naïve or undifferentiated state than matrigel.; the proliferation profile of NSCs shows a doubling time of 47.2 hours (panel C); differentiated NSCs after 7 days in differentiation medium are positive for Tuj1 (panel D), GFAP (panel E), and O4 (panel F); the differentiation of NSCs in UBM (U) and matrigel (M) was quantitatively measured by Western blot analyses (panel F) showing comparable expression of Tuj1 and GFAP. This finding suggests both neuronal and astrocytic differentiation in both matrices; r-tubulin was used as the loading control.

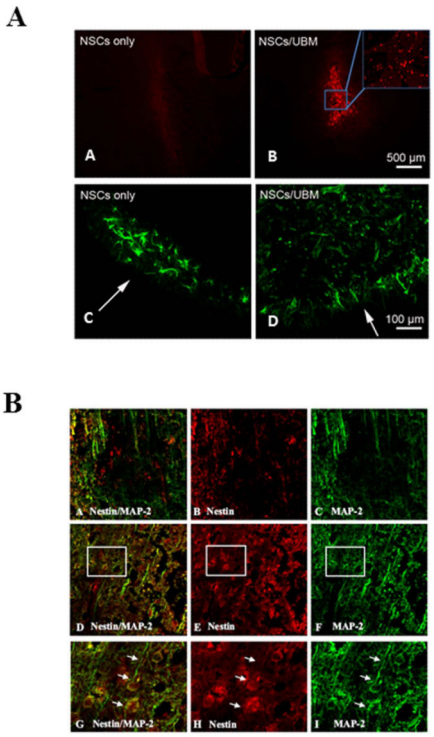

Figure 2. Characterization of NSC viability in rat cortex subjected to CCI

(A) NSCs in UBM survive 3 days after transplantation into rat brain *in vivo*. Representative confocal images of positive staining for BrdU (red) and nestin (green) show the distribution of injected exogenous NSCs and all NSCs. Low survivability of stem cells and limited penetration into brain parenchyma when only NSCs were injected (panel A and C); extended survival and parenchymal penetration of stem cells when NSCs were injected with UBM (panel B and D); (B) NSC survival and differentiation with or without UBM at 7 days post-CCI in rat brain. Representative confocal images of positive staining for nestin (red), MAP-2 (green) and merged signals indicate survival of NSCs (red) and neurites (green) when injected as NSC only (panels A–C) or NSCs in UBM (panels D–F). Magnified images corresponding to inset rectangles in panels D–F are illustrated in panels G–I. Arrows in G–I point to neurites growing from stem cells and indicate their *in vivo* differentiation.

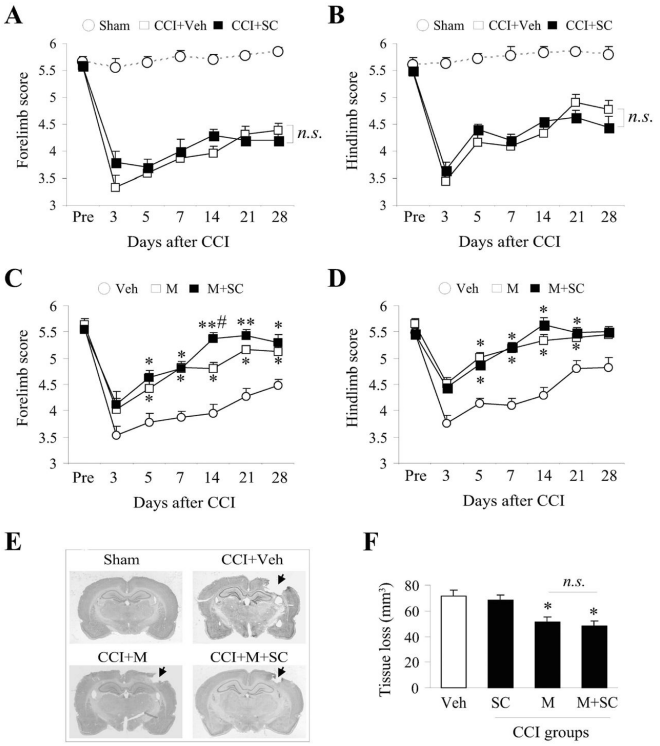

Figure 3. Transplantation of NSCs in UBM scaffold reduces motor deficits and tissue loss in rats subjected to CCI

Injections of vehicle, NSC only, UBM scaffold, or NSC in UBM scaffold (2.5μl, four injections along the rostrocaudal axis into the cortex or the dorsal hippocampus just above the pyramidal neuron layers of CA3) were performed 24 hours post-CCI. Motor function was evaluated via forelimb and hindlimb foot-fault tests pre-CCI and at 3, 5,7,14 21 and 28 days post-CCI. Injections of NSCs without a scaffold were unable to attenuate CCI-induced loss of motor function based on the scores from forelimb (A) and hindlimb (B) foot-fault tests; Injections with UBM scaffold alone and NSCs in UBM scaffold both decreased loss of motor function based on forelimb (C) and hindlimb (D) foot-fault tests; n=10/group. Data are presented as mean ± standard error, *p<0.05; **p<0.01 versus sham; #p<0.05 versus CCI + UBM only. Injections of UBM scaffold or NSCs in UBM scaffold reduced tissue loss from CCI compared to vehicle, as visualized by cresyl violet staining (E). Tissue loss was quantified and summed across serial cresyl violet-stained brain sections (F). UBM alone or with NSCs significantly reduced tissue loss compared to vehicle; n=10/group. Data are presented as mean ± standard error, *p<0.05; **p<0.01 versus CCI + vehicle.

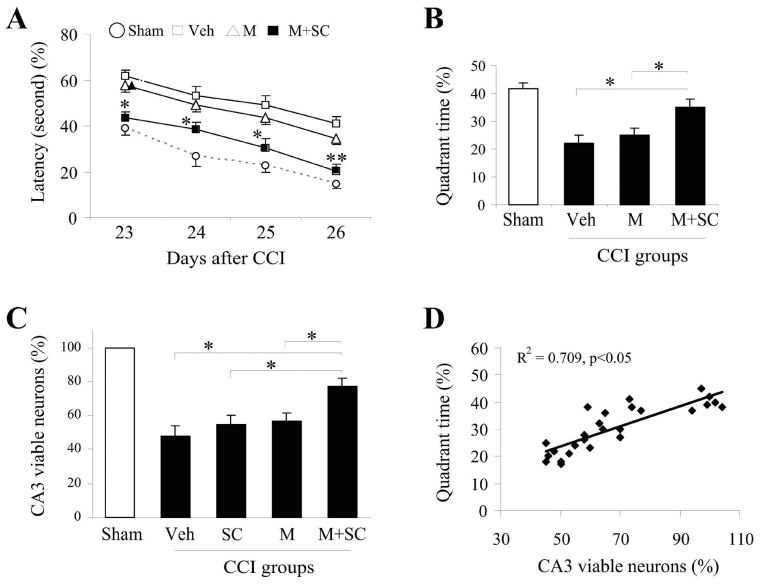

Figure 4. Transplantation of NSCs in UBM scaffold reduces memory and cognitive impairments and increases viable neurons in CA3 region of the hippocampus of rats subjected to CCI

Injections of vehicle, NSCs only, UBM scaffold or NSCs in UBM scaffold (2μ, five injections along the rostrocaudal axis into the cortex or the dorsal hippocampus just above the pyramidal neuron layers of CA3) were performed 24 hours post-CCI, and memory and cognitive function were evaluated daily by the Morris water maze test from 23–26 days post-CCI. Only injections with NSCs in UBM scaffold were able to ameliorate memory and cognitive deficits based on the decrease in latency to reach the target platform (A) and increase in time spent in the same quadrant as the submerged target platform (B); n=10/group. Data are presented as mean ± standard error, *$p<0.05$; **$p<0.01$ versus sham; #$p<0.05$ versus vehicle; (C) The number of viable neurons in the CA3 region of the hippocampus of rats from each group were counted and expressed as a fraction of sham controls. The results indicate that rats receiving NSCs in UBM have a significantly higher number of viable neurons than other treatment groups; n=10/group. Data are presented as mean ± standard error, *$p<0.05$ versus vehicle, NSC only, UBM alone respectively; (D) The time spent in the target quadrant is plotted against the number of viable neurons in the CA3 region to reveal the direct correlation between CA3 viability and memory and cognitive ability.

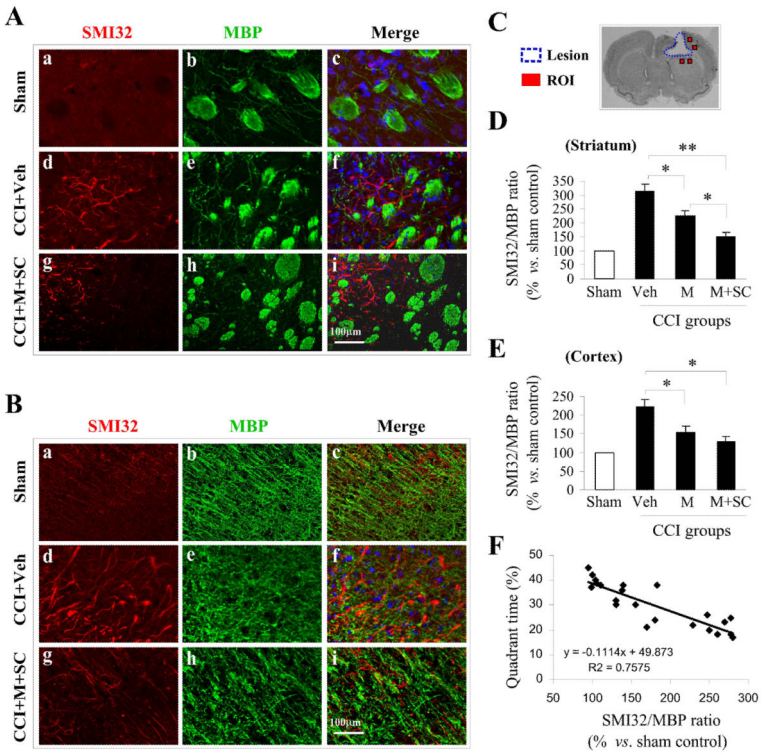

Figure 5. Transplantation of UBM alone or with NSCs attenuates white matter injury in rats subjected to CCI

Representative confocal images of the striatum (A) and cortex (B) stained for SMI32 (non-phosphorylated neurofilament protein, marker for white matter injury, red) and MBP (myelin basic protein, marker for mature oligodendrocytes, green) 28 days post-CCI in rats receiving vehicle (panels d–f) or NSCs in UBM scaffold (panels g–i) and in sham animals (panels a–c); (C) The location of regions of interest (ROI) around the CCI lesion are indicated as red squares, where the SM132/MBP ratio was calculated 28 days post-CCI. The SMI32/MBP ratio reflects the extent of white matter injury in the striatum (D) and cortex (E) of rats receiving vehicle, UBM only and NSCs in UBM. White matter injury was mitigated in rats receiving UBM alone and NSCs in UBM in both regions. The greater protective effect of NSCs in UBM reveals the additive nature of the protection against white matter injury; n=10/group. Data are presented as mean ± standard error, *p<0.05; **p<0.01 versus vehicle or UBM alone; (F) Time spent in the target quadrant was plotted against the SMI32/MBP ratio to reveal the correlation between the extent of white matter injury and memory and cognition.